NODE INTERPOLATION CELL METHOD FOR MULTISCALE MECHANICS ANALYSIS OF PERIODIC MATERIALS: ANALYSIS AND COMPARISON WITH FVDAM

Sheng ZHANG, Xiguang GAO*, Yingdong SONG

State Key Laboratory of Mechanics and Control of Mechanics Structure, College of Energy and Power Engineering and, Nanjing University of Astronautics and Aeronautics, 29 Yudao Street, Nanjing 210016, China
**Gaoxiguang@gmail.com*

Keywords: Composite materials, Micro-mechanics, FVDAM, Effective moduli

Abstract
In this paper, a node interpolation cell method (NICM) is developed for multiscale mechanics analysis of periodic materials. To accomplish this work, the displacement within the subcell is expanded in terms of the global strains and the fluctuating displacements. Then the stander FEM approach and the periodic boundary condition are employed to establish the relation between the global strain and local displacement. Using the homogenized method, the global stress is expressed as the function of global strain and the parameters of microstructure and the moduli of individual phase. Finally, the effective constitutive equations are derived from the relations between the global strain and the global stress. The difference between NICM and Finite Volume Direct Averaging Micromechanics (FVDAM) is discussed.

1. Introduction

Multiscale mechanics method that evaluates the effective mechanical properties and microscopic stress field of heterogeneous materials is becoming a much important method in present day engineering. The generalized method of cells (GMC) proposed by Paley and Aboudi (1992) is a recently developed micromechanics model for the response of multiphase materials with arbitrary periodic microstructure. The method employs a first-order representation of the displacement field in each subcell of the repeating unit cell, producing piece-wise uniform strain and stress fields throughout the cell. However, since the employment of first-order representation of displacement, the local stress field predicted by GMC is not as good (Aboudi et al., 1999).

In order to improve the accuracy of GMC, a high-order version of GMC is developed by Aboudi et al.(2001, 2003), Pindera et al. (2003), and Bednarcyk et al. (2004). The method is a significant improvement over GMC because it employs a second-order representations of stress and strain fields within the individual phase unlike the iso-strain and iso-stress approach of GMC. According to the character of high-fidelity representations of stress and strain fields, the high fidelity version of GMC is named High-Fidelity Generalized Method of Cell (HFGCM). HFGMC provides the necessary shear-coupling between the local normal and shear deformation fields and the macroscopically applied average strains. This feature produced excellent estimates of both the effective thermo-elastic moduli of periodic composites and the local stress and strain fields in the individual phases (Aboudi et al., 2001).

Bansal and Pindera (2005) demonstrate that the underlying framework of HFGMC is based on an approximate, and quite standard, elasticity approach involving direct volume-averaging of the subcell stress equilibrium equations in conjunction with the imposition of displacement and traction continuity conditions in a surface-average sense across adjacent subcell faces. By using the local/global stiffness matrix approach, they developed the efficient reformulation of HFGCM and suggest that HFGMC belongs to a category of finite-volume, direct averaging micromechanics (FVDAM) approaches.

Recently, FVDAM is expended to quadrilateral sub-volumes by incorporating parametric mapping technology (Cavalcante et al. 2006, 2007; Gattu 2007) or directly integral approach (GAO et al.), rather than the rectangular sub-volumes employed in the original theory. This expansion enables FVDAM more exact and more efficient modeling of unit cell's micro-structural details. However, despite the FVDAM's accuracy and efficiency in modeling the micro-structural details of material, the stress field predicted by FVDAM is still not good since too many average aspects are used in FVDAM, such as the average displacement and traction continuity conditions, the average equilibrium equations and the volume-averaged Jacobian of the coordinate transformation (Cavalcante, 2007). On the other hand, it is difficult to model actual three-dimensional microstructures with sufficient fidelity using the standard FVDAM, since the limitation of the present computing capabilities. In order to overcome the disadvantage mentioned above, a node interpolation cell method (NICM) is developed here.

2. The Theory for Node Interpolation Cell Method

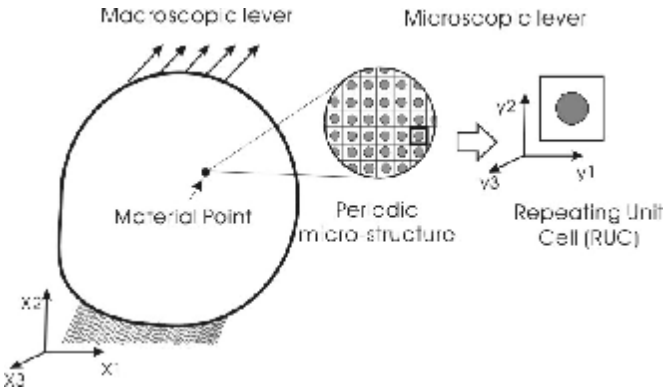

Fig.1 An illustration of a material with periodic microstructure

The multi-scale theory (Benssousan et al. 1987; Sanchez-Palencia 1980) is employed to derive the formulations of NICM. Within the domain of Repeating Unit Cell (RUC, seeing figure 1), the construction of the displacement field is based on the two scale expansion of the form

$$u_i(\mathbf{x},\mathbf{y}) = u_{0i}(\mathbf{x},\mathbf{y}) + d \cdot u_{1i}(\mathbf{x},\mathbf{y}) + d^2 \cdot u_{2i}(\mathbf{x},\mathbf{y}) + \mathbf{L} \qquad (1)$$

where $\mathbf{x} = (x_1, x_2, x_3)$ are the global or macroscopic coordinates, $\mathbf{y} = (y_1, y_2, y_3)$ are the local or microscopic coordinates defined with respect to the repeating unit cell, $u_{ji}(\mathbf{x},\mathbf{y})$ are y-periodic. The small parameter δ characterizes the size of the repeating unit cell and relates the microscale to macroscale by $\mathbf{y} = \mathbf{x}/d$. Combining the above displacement field representation with the relation $\mathbf{y} = \mathbf{x}/d$ between the two scales, the strain field is separated

into the average stains $\bar{e}_{ij}(\mathbf{x})$ and local strains $\hat{e}_{ij}(\mathbf{x})$, respectively:

$$e_{ij} = \bar{e}_{ij}(\mathbf{x}) + \hat{e}_{ij}(\mathbf{x},\mathbf{y}) + \mathbf{O}(d) \tag{2}$$

The average and local strains are derived by the corresponding displacement components $\bar{u}_i$ and $\hat{u}_i$, as

$$\bar{e}_{ij}(\mathbf{x}) = \frac{1}{2}\left(\frac{\partial \bar{u}_i}{\partial x_j} + \frac{\partial \bar{u}_j}{\partial x_i}\right), \hat{e}_{ij}(\mathbf{x},\mathbf{y}) = \frac{1}{2}\left(\frac{\partial \hat{u}_i}{\partial y_j} + \frac{\partial \hat{u}_j}{\partial y_i}\right) \tag{3}$$

Using the decomposition of the strains mentioned above, the displacement field representation is expressed in the form

$$u_i(\mathbf{x},\mathbf{y}) = \bar{e}_{ij}x_j + \hat{u}_i + \mathbf{O}(d^2) \tag{4}$$

where $\bar{e}_{ij}$ are the known or applied macroscopic strains. This form is employed in constructing an approximate displacement field for the solution of the multiscale problem. When δ is sufficient small, the affect of $\mathbf{O}(d^2)$ on the displacement can be ignored. Therefore,

$$u_i(\mathbf{x},\mathbf{y}) = \bar{e}_{ij}x_j + \hat{u}_i \tag{5}$$

Then the fluctuating displacements become the fundamental variables for every given global strains. In this paper, the stander FEM approach is employed to obtain the approximate solution of $\hat{u}_i$. If the effect of body force is ignored, the virtual work principle has the form (T.H.Richards, 1977):

$$\int_\Omega s_{ij}\,de_{ij}\,dv = \int_{S_s} T_i\,d\,u_i\,ds \tag{6}$$

where Ω stands for the domain of RUC, and S_s stands for the stress boundary. Substitution of (5) into (6) gives that:

$$\int_\Omega \left(E_{ijkl}\bar{e}_{kl}d\bar{e}_{ij} + E_{ijkl}\bar{e}_{kl}d\hat{e}_{ij} + E_{ijkl}\hat{e}_{kl}d\bar{e}_{ij} + E_{ijkl}\hat{e}_{kl}d\hat{e}_{ij}\right)dv = \int_{S_s}\left(T_i d\bar{e}_{ij}x_j + T_i d\hat{u}_i\right)ds \tag{7}$$

Where E_{ijkl} is the elastic tensor, $\hat{e}_{ij} = \frac{1}{2}\left(\hat{u}_{i,j} + \hat{u}_{j,i}\right)$.

In equation (7), we assume that the prescribed global strain keeps constant in the process of deformation. Therefore the variation of $\bar{e}_{ij}$ is equal to zero. Thus

$$\int_\Omega \left(E_{ijkl}\bar{e}_{kl}d\hat{e}_{ij} + E_{ijkl}\hat{e}_{kl}d\hat{e}_{ij}\right)dv = \int_{S_s} T_i d\hat{u}_i ds \tag{8}$$

In order to continue the analysis, the repeating unit cell highlighted in Fig. 1 is discretized into subcells designated by an integer (q). Then the multiscale virtual work principle is translated into discretized form

$$\sum_e \int_{e\Omega} \left(E_{ijkl} \bar{e}_{kl} d\hat{e}_{ij} + E_{ijkl} \hat{e}_{kl} d\hat{e}_{ij} \right) dv = \sum_e \int_{eS} T_i d\hat{u}_i ds \qquad (9)$$

where ${}^e\Omega$ denotes the domain of subcell, and ${}^eS$ denotes the boundary of subcell.
Within each subcells, the fluctuating displacement and variation of fluctuating displacement are approximated by linear combinations of their nodal values and their shape functions

$${}^e\hat{u}_i = {}^eN^p \, {}^e\hat{u}_i^p \quad d\,{}^e\hat{u}_i = {}^eN^p d\,{}^e\hat{u}_i^p \qquad (10)$$

The corresponding fluctuating strain has the form

$${}^e\hat{e}_{ij} = \frac{1}{2} {}^eN^p_{,j} \, {}^e\hat{u}_i^p + \frac{1}{2} {}^eN^p_{,i} \, {}^e\hat{u}_j^p \qquad (11)$$

where ${}^eN^p_{,j} = \dfrac{\partial {}^eN^p}{\partial x_j}$. Combination of (9), (10) and (11) gives that

$$\sum_e {}^e\hat{u}_k^q \, {}^eK_{kqip} d\,{}^e\hat{u}_i^p + \sum_e \bar{e}_{kl} \, {}^eC_{klip} d\,{}^e\hat{u}_i^p = \sum_e {}^eT_{ip} d\,{}^e\hat{u}_i^p \qquad (12)$$

where ${}^eK_{kqip} = \int_{e\Omega} K_{kqip} dv$, ${}^eC_{klip} = \frac{1}{2} \int_{e\Omega} \left(E_{ijkl} \, {}^eN^p_{,j} + E_{jikl} \, {}^eN^p_{,j} \right) dv$, ${}^eT_{ip} = \int_{eS} T_i \, {}^eN^p ds$ and

$$K_{kqip} = \frac{1}{4} E_{ijkl} \, {}^eN^q_{,l} \, {}^eN^p_{,j} + \frac{1}{4} E_{ijlk} \, {}^eN^q_{,l} \, {}^eN^p_{,j} + \frac{1}{4} E_{jikl} \, {}^eN^q_{,l} \, {}^eN^p_{,j} + \frac{1}{4} E_{jilk} \, {}^eN^q_{,l} \, {}^eN^p_{,j}$$

By imposing the periodic boundary conditions, the relation between global strains and nodal fluctuating displacement are given by the solutions of (12)

$${}^e\hat{u}_k^p = {}^eKC_{kpmn} \bar{e}_{mn} + {}^eU_k^p \qquad (13)$$

where ${}^eKC_{kpmn}$ is the component of a four order tensor. It is the function of the moduli and geometrical parameters of subcell. ${}^eU_k^p$ is the component of a two order tenser, which is related to the stress boundary conditions.
Based on the usually used homogenization approach (Michel, 1999), the global stresses are defined as the integral of local stresses throughout the RUC.

$$\bar{s}_{ij} = \frac{1}{V} \int_\Omega s_{ij} dv \qquad (14)$$

By using the discretization, the integral are performed within each subcells

$$\bar{s}_{ij} = \frac{1}{V} \sum_e \frac{{}^eV \, {}^eE_{ijkl}}{{}^eV} \int_{e\Omega} {}^e e_{kl} dv \qquad (15)$$

Thus

$$\bar{s}_{ij} = \sum_e \frac{{}^eV}{V} \left({}^eE_{ijkl} \bar{e}_{kl} + {}^eE_{ijmn} \, {}^e\bar{N}^p_{,n} \, {}^eKC_{mpkl} \bar{e}_{kl} + {}^eE_{ijkl} \, {}^e\bar{N}^p_{,l} \, {}^eU_k^p \right) \qquad (16)$$

where ${}^e\bar{N}^p_{,l} = \frac{1}{{}^eV}\int_{{}^e\Omega} {}^eN^p_{,l}\,dv$.

Simplification of equation (16) gives that

$$\bar{s}_{ij} = \bar{E}_{ijkl}\bar{e}_{kl} + \bar{T}_{ij} \tag{17}$$

where $\bar{E}_{ijkl} = \sum_e \frac{{}^eV}{V}\left({}^eE_{ijkl} + {}^eE_{ijmn}\,{}^e\bar{N}^p_{,n}\,{}^eKC_{mpkl}\right)$ and $\bar{T}_{ij} = \sum_e \frac{{}^eV}{V}\left({}^eE_{ijkl}\,{}^e\bar{N}^p_{,l}\,{}^eU^p_k\right)$

By using the formulations derived herein, the local stresses and the global elastic moduli of the heterogeneous material for prescript global strains can be estimated conveniently.

3. Numerical results and discussion

Herein, we test NICM's efficiency and accuracy by determining local stress field of a unidirectional composite, with a square array of fibers in the x_2-x_3 plane, seeing fig 1. Figure 2 shows the mesh of RUC with fiber volume fraction of 0.47 for both FVDAM and NICM. The fiber and the matrix phases are both isotropic. The elastic Young's moduli and Poisson's ratio of carbon fiber and SiC matrix are 230(GPa), 430(GPa), 0.25 and 0.2. When the prescript transverse global strain $\bar{e}_{22}$ is equal to 0.01%, the local transverse stress $\bar{s}_{22}$ predicted by NICM along the boundary between subcell A and B is shown in finger 3.

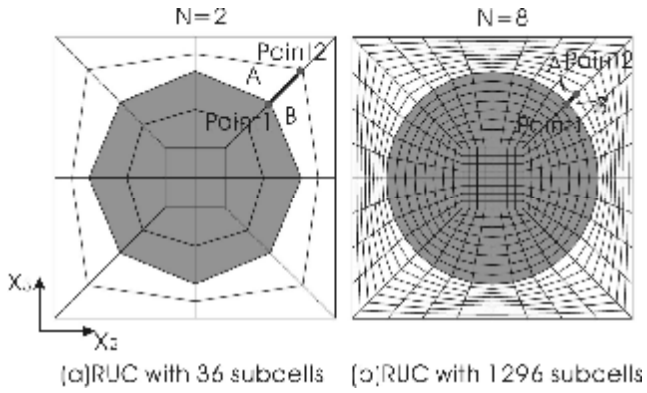

Fig.2 The discretization employed by NICM and FVDAM

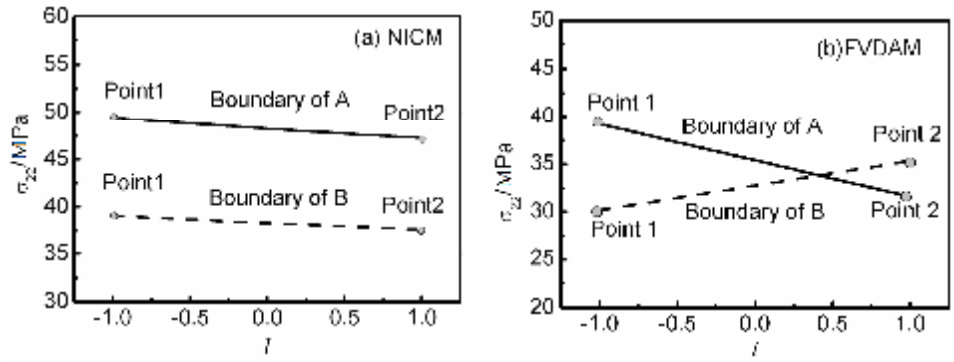

Fig. 3 The distribution of stresses along the boundary between subcell A and B: (a) NICM, (b) FVDAM

Figure 3 shows that the stress predicted both by FVDAM and NICM distribute linearly along the boundary and that the stresses are discontinuous at the boundary. In the case of FVDAM, the stress continuity is imposed by enforcing the continuity of surface-average tractions as presented by following equation (GAO et al.).

$$\bar{T}_i^+ + \bar{T}_i^- = 0 \tag{18}$$

where $\bar{T}_i^+$ and $\bar{T}_i^-$ are the average tractions at the common boundary of adjacent subcells. Since the stresses distribute linearly along the boundary, equation (18) means the continuity of traction at the center of subcells' boundary, seeing figure 4.

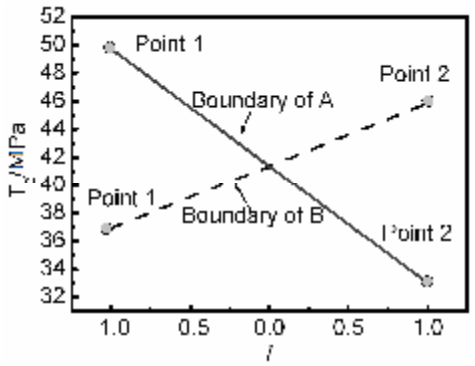

Fig.4 The distribution of traction predicted by FVDAM along the boundary between subcell A and B

However, since the traction is the combination of normal and shear stresses through Cauchy's relations, the continuity of average traction can not ensure the continuity of average stresses, and therefore leads to an offset of stresses at the interface of subcells, which has been verified by figure 3b. Both NICM and FVDAM belong to the category of numerical technology. The quantity of mesh is an important factor which affects the accuracy of result. In order to investigate the effect of mesh size on the results predicted by FVDAM and NICM, a RUC with 1296 subcells are considered in present analysis, seeing figure2b. The stresses predicted by FVDAM and NICM along the boundary are shown in figure 5, which is compared with the result with 36 subcells.

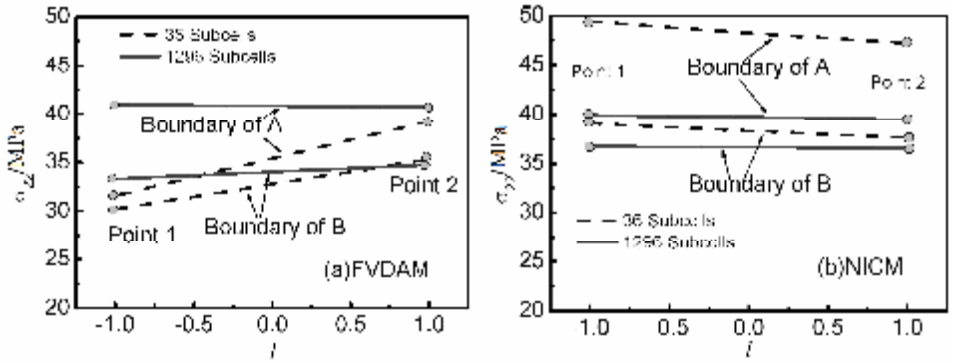

Fig. 5 Comparison of the distribution of σ_{22} based on the 36 subcell discretization with the results based on the 1296 subcell discretization: (a) FVDAM, (b) NICM

The results presented in figure 5 indicate that in contrast with the RUC with 36 subcells the continuity of stresses predicted by NICM is improved in the case of the RUC with 1296 subcells, while the continuity of stresses predicted by FVDAM can not be improved by refining the mesh. This feature of FVDAM will result in a stress distribution with many pieces as presented in figure 6. In order to obtain a more continuous stresses distribution, more subcells should be employed to mimic the microstructure of material as discussed by Cavalcante (2007). Since the continuity of stress predicted by NICM is improved with the refine mesh, the stress distribution is better than FVDAM, which is proved by the comparison presented in figure 6.

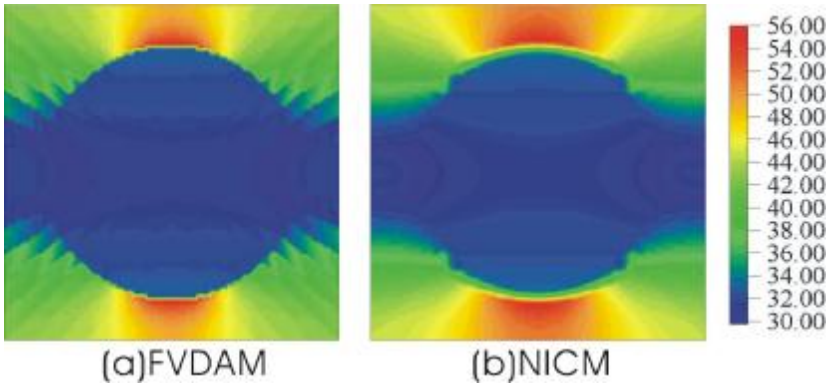

Fig. 6 Local σ_{22} stress (MPa) distribution in the region of RUC, Comparison of the FVDAM result with NICM result: (a) FVDAM, (b) NICM

In this section, the efficiency of NICM is also compared with FVDAM. The time used by two methods for analysis is shown in figure 7, where the transverse axes is the number of subcells along the boundary of RUC. The comparison indicates that NICM take less time than FVDAM to perform the same analysis. This is the result of less unknown variable appears in the NICM's mesh than FVDAM's mesh. Although both methods employ the same subcell discretization, the total number of unknown variable of NICM is equal to 3Nq, where Nq is the number of nodes. In the case of FVDAM, the total number of unknown variable is equal to 3Np, where Np is the number of subcell's boundary. Since each nods belongs to four subcells for most case, one subcell take up only one node, thus Nq≈N, where N is the number of subcells. Similarly, we can conclude that Np≈2N. The number of unknown variable of NICM is about half of the FVDAM. Therefore, NICM is more efficient than FVDAM. This feature makes NICM easier than FVDAM to expand to three-dimension problems.

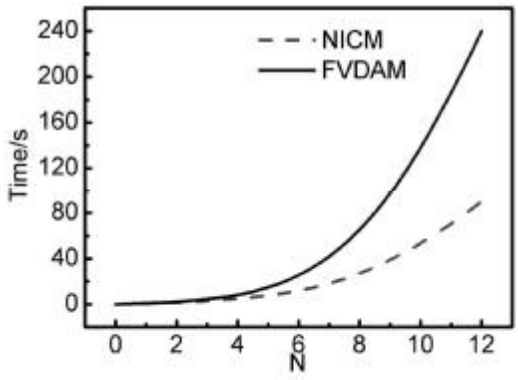

Fig. 7 Comparison of efficiency between NICM and FVDAM

4. Conclusion

Using the homogenized method, we derived the formulations of effective elastic moduli of the materials. The local stresses distribution is computed for a unidirectional fiber reinforced composite with periodic microstructure, and compared with the corresponding results predicted by FVDAM. The results indicate that (1) the stress predicted both by FVDAM and NICM distribute linearly along the subcell interface and that the stresses are discontinuous at the interface, (2) by refining the mesh, the continuity of stresses predicted by NICM is improved while the FVDAM predictions of the stress fields exhibit slight discontinuities in the matrix phase away from the fiber/matrix interface, (3) the total number of unknown variables of NICM is much less than FVDAM for the same mesh, which lead to approximately 50% reduction in the global system of equations compared to the FVDAM.

Acknowledgement

The works presented in this paper is supported by the National Natural Science Foundation of China (No.51075204, No. 51105195) and Aeronautical Science Foundation of China (No. 2011ZB52024).

Reference

[1] Aboudi, J., Pindera M-J., Arnold, S M. Higher-order theory for functionally graded materials. *Composites Part B*, 33, pp. 777-832(1999)

[2] Aboudi, J., Pindera, M-J., and Arnold, S.M. Linear Thermoelastic Higher-Order Theory for Periodic Multiphase Materials. *Journal of Applied Mechanics*, 68, pp. 697-707(2001).

[3] Aboudi, J., Pindera, M-J, and Arnold, S.M. Higher-Order Theory for Periodic Multiphase Materials with Inelastic Phases. *International Journal of Plasticity*, 19, pp. 805-847(2003).

[4] Anthony Drago, Marek-Jerzy Pindera Micro-macromechanical analysis of heterogeneous materials: Macroscopically homogeneous vs periodic microstructures. *Composite Science and Technology*, 67, pp. 1243-1263(2007).

[5] Bansal,Y., and Pindera, M-J. A Second Look at the Higher-Order Theory for Periodic Multiphase Materials. *Journal of Applied Mechanics*, 72, pp. 177-195(2005).

[6] Bednarcyk, B.A., Arnold, S.M., Aboudi, J., and Pindera, M-J. Local Field Effects in Titanium Matrix Composites Subject to Fiber-Matrix Debonding. *International Journal of Plasticity*, 20, pp. 1707-1737(2004).

[7] Benssousan, A., Lions, J.-L., Papanicolaou, G. *Asymptotic Analysis for Periodic Structures*. North-Holland Publishing Company, Amsterdam (1978).

[8] Cavalcante, M.A.A. *Modeling of the transient thermo-mechanical behavior of composite material structures by the finite-volume theory*. MS Thesis. Civil Engineering Department. Federal University of Alagoas, Maceio, Alagoas, Brazil (2006).

[9] Cavalcante, M.A.A., Marques, S.P.C., Pindera, M-J. Parametric Formulation of the Finite-Volume Theory for Functionally Graded Materials. Part I: Analysis. *Journal of Applied Mechanics*, 74, pp.935-945 (2007).

[10] Cavalcante, M.A.A., Marques, S.P.C., Pindera, M-J. Parametric Formulation of the Finite-Volume Theory for Functionally Graded Materials. Part II: Numerical Results. *Journal of Applied Mechanics*, 74, pp.946-957 (2007).

[11] Gattu, M. *Parametric Finite Volume Theory for Periodic Heterogeneous Materials*. MS Thesis, Civil Engineering Department, University of Virginia (2007)

[12] Michel J.C., H.Moulinec, P.Suquet. Effective properties of composite materials with periodic microstructure: a computational approach. *Computer methods in applied mechanics and engineering*, 172, pp. 109-143(1999).

[13] Paley, M., and Aboudi, J. Micromechanical Analysis of Composites by the Generalized Method of Cells. *Mechanics of Material*, 14, pp. 127-139(1992).

[14] Pindera, M-J., Aboudi, J., and Arnold, S.M. Analysis of Locally Irregular Composites Using High-Fidelity Generalized Method of Cells. *AIAA Journal*, 44, pp. 2331-2340(2003).

[15] Richards T.H. *Energy methods in stress analysis*, Ellis Horwood Publishing Company, Chichester, U.K. (1977)

[16] Sanchez-Palencia, E. *Lecture Notes in Physics 127: Non-homogeneous Media and Vibration Theory*. Springer-Verlag Publish Company, Berlin (1980)

[17] Xiguang, GAO, Yingdong, SONG, Zhigang, SUN, Quadrilateral Subcell Based Finite-Volume Micromechanics Theory for Multiscale Analysis of Elastic Periodic Materials, *Journal of applied mechanics*, 76, pp. 011013-1-011013-7